IEEE Access
Multidisciplinary ⋮ Rapid Review ⋮ Open Access Journal

Received March 19, 2022, accepted March 31, 2022, date of publication April 11, 2022, date of current version April 27, 2022.

Digital Object Identifier 10.1109/ACCESS.2022.3166516

Drone Assisted Network Coded Cooperation With Energy Harvesting: Strengthening the Lifespan of the Wireless Networks

PANKAJ KUMAR[1], SAGNIK BHATTACHARYYA[2], (Graduate Student Member, IEEE), SAM DARSHI[2], (Senior Member, IEEE), ASHWANI SHARMA[2], (Member, IEEE), AKRAM A. ALMOHAMMEDI[3,4], VLADIMIR SHEPELEV[3], AND SAMAR SHAILENDRA[5], (Senior Member, IEEE)

[1]Department of Electronics and Communication Engineering, Netaji Subhas University of Technology, Dwarka, Delhi 110078, India
[2]Department of Electrical Engineering, Indian Institute of Technology Ropar, Rupnagar, Punjab 140001, India
[3]Automobile Transportation Department, South Ural State University, 454080 Chelyabinsk, Russia
[4]Electrical and Electronic Engineering Department, Karabük University, 78050 Karabük, Turkey
[5]Intel Technology, Bengaluru 560037, India

Corresponding authors: Sam Darshi (sam@iitrpr.ac.in) and Akram A. Almohammedi (akrama2810@gmail.com)

This work was supported in part by the Science & Engineering Research Board (SERB), Government of India, under Grant CRG/2021/007002.

ABSTRACT Next generation wireless systems include battery operated devices which demand higher throughput and a better reliability in an energy efficient fashion. To fulfil these requirements, in this paper, we propose a novel scenario where we include a dynamic Wireless Power Splitting (WPS) factor for Energy Harvesting (EH) at nodes in a Drone Assisted Network Coded Cooperation (DA-NCC) system. The dynamic WPS factor used for EH in DA-NCC system is made more realistic by determining through the probability of Line-of-Sight (LoS) occurrence. Analytical framework is developed for residual Analog Network Coding (ANC) noise and variance of ANC-noise in EH scenario. We also derive the average rate and average outage probability expressions for the proposed channel model. Various algorithms are developed for deciding the Air-to-Ground (A2G) channel distributions, harvesting the energy at relay and source nodes and evaluating the performance metrics of our proposed work. Our investigations reveal that the use of EH in DA-NCC improves the lifespan of the network. Our findings play important roles in disaster management scenarios where cellular connections to base stations are disrupted due to natural calamities and battery constrained drones are deployed for assistance.

INDEX TERMS UAV/drone, multi-user cooperation, network coding, energy harvesting, wireless power splitting, outage probability, Rayleigh channel, Rician channel, statistical channel model.

I. INTRODUCTION

The demand for higher throughput and better reliability is increasing each day among wireless users. To achieve reliability easily, the concept of Cooperative Communication (CC) was introduced where each source-destination pair is aided by a relay and a total of $2N$ time-slots are required [1]. On the other hand, to achieve a higher throughput, the concept of Network Coding (NC) was introduced [2]. In a typical NC network, intermediate relay nodes combine the received signals and transmit it together thus, saving broadcasting time-slots and improving the throughput. To further meet the ever increasing demands, researchers merged NC with CC to form Network Coded Cooperation (NCC) which aims to exploit the advantages of CC and NC at one go [3], [4]. In a typical NCC system, participating sources transmit using a Time Division Multiple Access (TDMA) protocol following which the relay transmits a superposed composite data. Thus, NCC requires a total of $N+1$ time-slots compared to $2N$ time-slots in the case of CC only. However, the performance of NCC is limited by the NC-noise that occurs during the extraction of the second copy of the desired signal at the destination node. Authors in [3] discussed the concept of NCC, however, given the static position of

The associate editor coordinating the review of this manuscript and approving it for publication was Yang Tang.

a ground relay providing reliability in a disaster scenario becomes a tangible task. In order to provide a reliable and faster mode of communication during disaster/post disaster scenario, authors in [5] introduced the usage of drone as a relay in a NCC system. This in turn provides a higher QoS for end users in disaster scenarios as it provides a greater LoS and thus, increased reliability. However, a probability based DA-NCC scenario is still an unmapped area which can provide a better accuracy to evaluate the performance.

Another important aspect of state-of-the-art energy-constrained wireless networks is the power consumption of battery operated wireless devices. Thus, conserving/harvesting energy in such cases must be of great importance not only to users but also to network designers. Extracting energy from the surrounding environment, is called EH. Devices can easily harvest energy from renewable energy sources like solar power, thermal power, wind power etc. which are effective both in terms of power and battery life. However, these kind of uncontrollable natural energy sources do not guarantee a constant source of energy, thus putting systems relying on these sources in jeopardy. To overcome this problem, EH from ambient Radio Frequency (RF) signals have caught the attention of researchers [6], [7]. Such signals not only carry information but also act as a source of energy for users which is referred to as wireless power transfer [8], [9]. This concept has generated considerable interest among researchers in the so-called Simultaneous Wireless Information and Power Transfer (SWIPT) network community. In SWIPT, the energy and information transfer take place at the same time and the relay uses a WPS factor for allocating the power to EH as well as to information. In [10]–[12], the analysis has been carried out by taking fixed WPS factor at relay node. Authors in [13] propose a dynamic scenario, where the relay optimizes the splitting factors based on the local channel condition. In [14], a new time switching protocol is proposed which is an amalgamation of time switching (TS) and adaptive power splitting (APS). To the best of the authors' knowledge, current works do not include a statistical dynamic channel based WPS factor for EH which considers the probability of occurrence of LoS/NLoS between the source and relay.

Now, as mentioned before, a drone based network needs appropriate A2G channel modelling for evaluating the accurate network performance. In case of a DA-NCC system, modelling of accurate A2G channels are advantageous because links associated with other nodes also contribute to the performance of the desired node. In the existing works discussed in Section II, A2G links are either modelled as Rayleigh or Rician distributed. However in reality, the A2G links between drone and transmitting nodes and between drone and receiving nodes may differ because of different locations, different obstacles etc. For example, in a multi-user scenario as shown in Fig. 1, uplink may be dominated by LoS component while the downlink may be dominated by Non-Line-of-Sight (NLoS) component. In such scenarios, the links dominated by LoS component may be modelled as Rician distributed while the others as Rayleigh distributed. Thus, the accurate channel assignment among A2G nodes is useful during the allocation of dynamic WPS factors for EH at relay node based on probability of occurrence of LoS and fixed EH at source nodes which has not be designed previously.

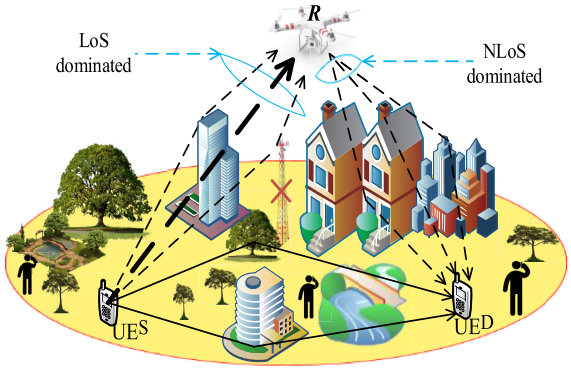

FIGURE 1. Illustration of drone (aerial relay) based CC with different channel conditions due to impediments in $UE^S - R$ and $R - UE^D$ channels. The $UE^S - R$ link, in particular, is dominated by LoS component (which can be modelled using the Rician distribution), while the $R - UE^D$ link is dominated by NLoS component (may be modelled by Rayleigh distribution).

Contribution: This work proposes the notion of probability based statistical channel modelling along with EH for DA-NCC system for an accurate channel characterization and strengthening the battery life. Based on the probability of occurrence of LoS/NLoS ($\mathbb{P}_L/\mathbb{P}_{NL}$), various A2G links are assigned either Rayleigh (NLoS) or Rician (LoS) distribution and accordingly a dynamic WPS factor is calculated based on probability of occurrence of LoS/NLoS.

The important contributions of this work are as follows:

1) Introduction of the concept of EH in a DA-NCC scenario and provide an analytical model for calculating harvested energy at relay and source nodes.
2) Introduction of a channel dependent WPS factor for EH at relay which varies on the probability of occurrence of LoS/NLoS and it's effects on the system performance. Also, the model considers a fixed WPS factor ($\rho = 1$) for sources.
3) Evaluating the system performance by considering the drone height and WPS factor as parameters which are based on the probability of occurrence of LoS/NLoS.
4) Derivation of ANC-noise and variance of the ANC-noise in EH scenario for DA-NCC system.

The rest of the paper is arranged as follows: Section II includes related work and motivation. Section III elucidates the system model which include probabilistic approach for channel assignment, EH from the RF at R signals and frame format for the availability of CSI at source and relay node. Section IV includes the analytical framework of the considered scenario. Section V includes the formulation of average rate and average outage probability. Results are discussed in the penultimate section, Section VI whereas Section VII concludes the paper.

II. RELATED WORK AND MOTIVATION

Most of the existing works related to UAV/drone assisted scenarios have a static approach for modelling the A2G channels. In [5], the authors derived the closed form expression of the outage probability by considering Rayleigh fading in the disaster scenario where the base station is disrupted. UAV with underlaid Device-to-Device (D2D) communications is considered in [15], in which authors derived the analytical framework for the coverage and rate using A2G links as Rayleigh distributed. Angle dependent Rician fading channel between A2G links is considered in [16], [17]. In [18], authors considered Rayleigh fading among Ground Users (GUs) while a piecewise function is proposed to approximate the probability of LoS for the A2G links. Performance evaluation of UAV assisted cooperative diversity is introduced in [19] by considering A2G links as Rician distributed. Probability-based assignment of A2G links is considered in [20] for drone based CC by considering height independent path loss exponent as well as Rician factor. The above studies considered only fixed A2G channel (Rayleigh or Rician) assignment model between drone and GUs. This leaves a huge unmapped area of dynamic channel modelling of multiple uplink/downlink cases based on probability of occurrence of LoS for drone based networks.

Another major concern for the next generation wireless networks is EH, which is not yet addressed considerably for NCC like multi-source multi-destination scenario in the existing literature. Few literature works are available related to CC that considered EH at relay node. In [21], authors analysed the performance of dual-hop relaying system with EH, considering log-normal channel distribution and Amplify-and-Forward (AF) or Decode-and-Forward (DF) as relaying scheme. In [22], a typical NC network is discussed, in which the relay node harvests energy from wireless transmissions and calculates the probability of successful data exchange and network lifetime gain. EH with incremental relaying in CC is considered in [23] and the expressions of throughput and outage are derived. The overall throughput of self-energized UAV assisted CC is improved in [24] by the use of Full-Duplex (FD) and DF based relaying scheme. In [25], EH in CC is considered in the presence of an eavesdropper where relay node works in FD mode. In [26], EH aided CC is discussed under Rayleigh faded channel conditions and derived the closed form expression of outage probability. Harvest-use-store power splitting with distributed beamforming is considered in [27] for wireless powered multi-relay CC network. Throughput maximization for UAV assisted CC is considered in [28], using time-sharing and power splitting information scheme at UAV. In [29], authors considered power splitting scheme for harvesting the energy at UAV and time switching protocol is used for relaying the information towards the GUs. Authors in [13], [14] derived the closed form expressions of the outage probability of the considered scheme and discuss the effective transmission rate. The model considered by authors in [30] and [31] aim to maximize the overall SNR of the CC system by proposing an adaptive power splitting protocol. To enhance the harvested energy, authors in [32] have also proposed a dynamic power split receiver and proposed moving the Information Decoding load to a different circuitry. However, the above cited works mostly considers a system with a dynamic WPS. Apart from incorporating a EH model in DA-NCC scenario, in the proposed proposed work, we also aim to determine the energy harvesting factor not just dynamically but also change it statistically with respect to the probability of occurrence of LoS thus making it more malleable for devices like drones.

To this end, we found that the existing literatures deals with the performance of three node configuration (cooperative communication) by considering EH (having dynamic WPS) along with fixed A2G channel (Rayleigh or Rician) model. However, in a practical scenario, such as urban or dense urban environments (high rise urban environment) the A2G channels among sources to drone and drone to destinations are different with different path loss exponent and Rician factor which changes in accordance with the drone height. In such a scenario, the dynamic WPS factor also depends on environments type as well as drone height. This concern motivates us to propose and investigate the channel dependent statistical WPS factor for EH at relay using the probability-based approach for assigning the channel between drone and GUs. To the best of our knowledge, this is the first work investigating the performance of drone assisted network comprising of multiple uplinks/downlinks using probability based statistical channel model along with channel dependent statistical WPS factor for EH at drone and fixed WPS factor for EH at source nodes. For developing the analytical framework of DA-NCC, AF relaying scheme is considered at the drone and Maximal Ratio Combining (MRC) is

TABLE 1. Summary of notations.

Symbol	Definition
N	Number of source-destination (S-D) pairs
R	Relay node
UEs	User equipments
x_i	Transmitted signal by i^{th} node
d_{ij}	Distance between i^{th} and j^{th} node
$\hbar_{ij}$	Channel coefficient between i^{th} and j^{th} node
η_i	Background noise at i^{th} node
σ_i^2	Variance of the background noise at i^{th} node
$\mathcal{P}_i$	Transmitted power by i^{th} node
$\mathcal{Y}_{ij}$	Signal received at j^{th} node transmitted by i^{th} node
$\sigma_{\mathcal{N}_i}^2$	Variance of the ANC-noise at i^{th} node
Γ_{ij}	SNR between i^{th} and j^{th} node
α	Path loss exponent
θ	Angle between d_j and r_j (shown in Fig. 2(b))
h_D	Drone height
η	EH efficiency
ρ	Power splitting factor
η_c	Signal processing noise

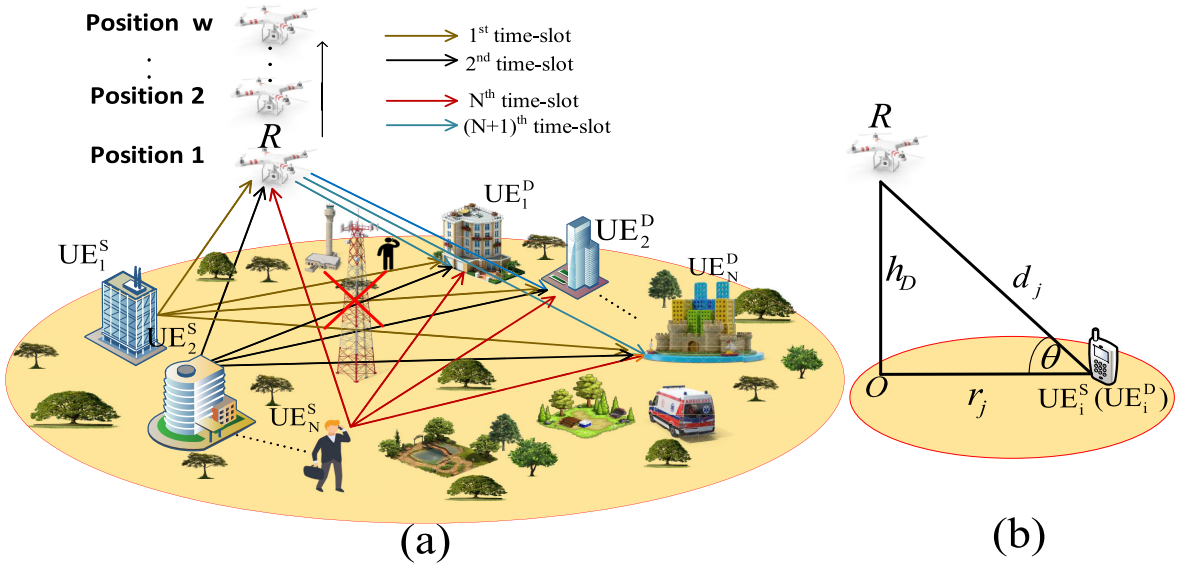

FIGURE 2. (a) Generalized scenario for DA-NCC system, where $UE_{i\in\{1,2,...N\}}^{S}$, UE_i^D, and R denote source, destination and relay (drone) nodes, respectively, (b) Height of R from O (h_D), distance between UE_i^S (UE_i^D) and O (r_j), and distance between UE_i^S (UE_i^D) and R (d_j) are depicted in this figure.

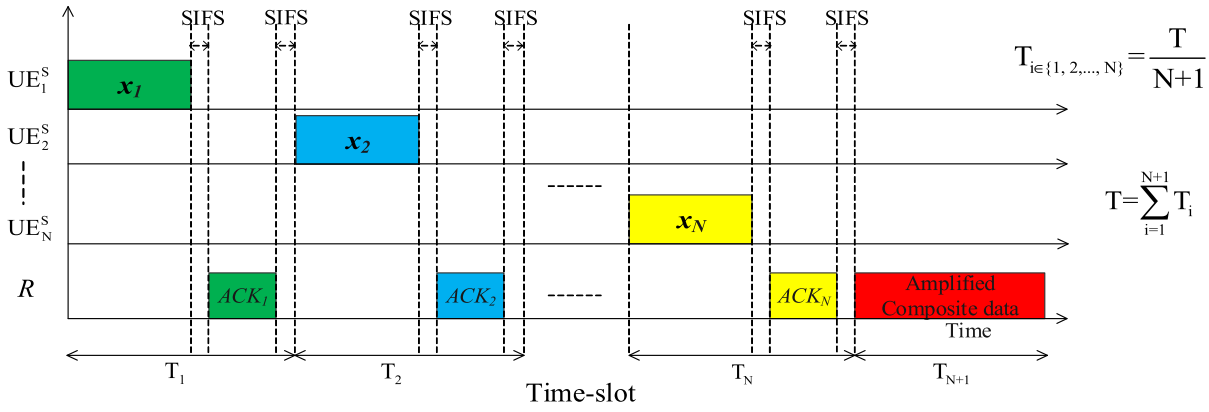

FIGURE 3. TDMA based MAC representation of DA-NCC system, where SIFS and T denote short inter-frame space and time duration for one communication cycle, respectively.

considered at destination nodes. Table 1 lists the notations and symbols used in this paper.

III. SYSTEM MODEL

We consider a generalized scenario comprising of N source UE-destination UE ($UE_{i\in\{1,2,...N\}}^{S} - UE_i^D$) pairs in the network as illustrated in Fig. 2(a). The $UE_i^S - UE_i^D$ pairs are assisted by a drone which acts as the relay (R) node. Distance between UE_i^S (UE_i^D) and R can be calculated by using $d_j = \sqrt{h_D^2 + r_j^2}$ as shown in Fig. 2(b). Elevation angle between R and UE_i^S (UE_i^D) is denoted by theta (θ). Transmission and reception of data in DA-NCC for N number of $UE_i^S - UE_i^D$ pairs are discussed as shown in Fig. 2(a). Here, each UE_i^S is assigned an orthogonal (TDMA) time-slot for transmitting it's data. Transmission of each UE_i^S is received by the corresponding UE_i^D as well as R and overheard by other $UE_{j\neq i,j\in\{1,2,..,N\}}^{D}$ nodes. R performs NC over the signals it received till N^{th} time-slot and sends an amplified composite data to all the UE_i^D nodes by using AF relaying scheme in $(N+1)^{th}$ time-slot. Thus, a total of $N+1$ time-slots are required to complete one communication cycle (Includes transmission by all $UE_{i\in\{1,2,..,N\}}^{S}$ and R nodes) of data transmission. The transmission of data from UE_i^S in orthogonal time-slots followed by the transmission of *ACK* frame from R is shown in Fig. 3. To achieve diversity, each UE_i^D tries to extract the 2^{nd} copy of the desired signal by subtracting the overheard signals received from the $UE_{j\neq i}^{S}$ and R node.

In this work, it is assumed that nodes[1] (UE_i^S, UE_i^D, R) are static during one communication cycle of data transmission. However, between two communication cycles, drone

[1]Each node is equipped with only one antenna and operates in half duplex mode.

(vertical) movement may be significant. Since, $UE_i^S - UE_i^D$ nodes are on the ground, the direct link between them may be obstructed by the obstacles for majority of time. As a result, a radio link between them is assumed to have only NLoS components. Although, due to the vertical movement of R, links among UE_i^S to R and R to UE_i^D may be dominated by either LoS or NLoS component. Therefore, these links are modelled using probabilistic channel model. To model the effects of LoS and NLoS components, Rician and Rayleigh fading[2] are used, respectively. Energy-related issues for the operation of drone movement have not been considered here. Each transmitting node has the same packet size and transmit the data at a fixed data rate. The processing power required by the relay's transmit/receive circuitry is presumed to be small in comparison to the power required for signal transmission from the relay to the destinations. For the DA-NCC system, in-band RF energy harvesting is being considered. As a result, the relay node can collect RF energy in the same frequency spectrum as data transmission. The friis equation with height dependent path loss exponent can be used to determine the collected RF energy from a transmitter in A2G space. During the development of the analytical framework, nodes working as UE_i^S and as UE_i^D are represented by source (S_i) and destination (D_i), respectively.

A. ENERGY HARVESTING FOR DRONE ASSISTED NETWORK CODED COOPERATION

In this subsection, we consider EH for the proposed DA-NCC system at R and S_i nodes, as explained below:

1) ENERGY HARVESTING AT RELAY NODE

Block diagram for Power Splitting Relaying (PSR) protocol is illustrated in Fig. 4. In Fig. 4 we see that $\mathcal{Y}_{S_iR}$ is the received signal at the power splitter PS. Here, PS divides the signal into two parts. The first part is denoted by $\sqrt{\rho_i}\mathcal{Y}_{S_iR}$ which is used for EH. The extracted energy is stored in battery[3] and later used by R for amplifying the coded signal, while the latter part of signal power is denoted by $\sqrt{(1-\rho_i)}\mathcal{Y}_{S_iR}$ which is associated with information signal. In the 1^{st} N time-slots, R allocates a portion of the received signal power ($\rho_i\mathcal{P}_{S_i\in\{1,2,..,N\}}$) to EH. The remaining power ($(1-\rho_i)\mathcal{P}_{S_i}$) is used for Information Transmission (IT), where $0 \leq \rho_i \leq 1$ is the power splitting factor. Here, η_c denotes signal processing noise. In the $(N+1)^{th}$ time-slot, R amplifies the coded information signal by using relay power and broadcasts it towards destination nodes.

2) POWER SPLITTING FACTOR

As discussed before, most of the current work consider the WPS factor to be static. On the other hand, in few works (related to CC) authors take a dynamic approach towards setting the WPS factor where they base their calculation on the channel gain. However, the introduction of EH and probability based LoS/NLoS is something which is still unmapped in the field of DA-NCC. This gives us the opportunity to design the WPS factor (ρ) to be statistically dynamic in nature based on probability of occurrence of LoS/NLoS between the source and relay. In this section, we thus propose a statistical dynamic approach for the WPS factor which changes based on LoS/NLoS. By using the proposed channel model (explained further in Section III-B), the average value of power splitting factor at R node may be calculated as

$$\rho^{\text{avg}} = \mathbb{P}_L\rho^{\text{Ric}} + \mathbb{P}_{NL}\rho^{\text{Ray}} \tag{1}$$

where $\mathbb{P}_L$ and $\mathbb{P}_{NL}$ denote the probability of occurrence of LoS and NLoS, respectively. ρ^{Ric} and ρ^{Ray} denote the power splitting factor for Rician and Rayleigh fading, respectively. The value of ρ^{Ray} and ρ^{Ric} can be calculated by using the following proposed formulas

$$\begin{aligned}\rho^{\text{Ray}} &= \Psi\left(1 - e^{-\frac{\text{SNR}_i}{\text{SNR}_{\text{avg}}}}\right)\\ \rho^{\text{Ric}} &= \Psi\left(1 - Q_1\left(\sqrt{2M}, \sqrt{2[1+M]\frac{\text{SNR}_i}{\text{SNR}_{\text{avg}}}}\right)\right).\end{aligned} \tag{2}$$

The genesis of proposing these formulas is that the dynamic WPS factor may not exceed 1. Therefore, we can formulate the expression of ρ in terms of the Cumulative Distribution Function (CDF). Since the CDF of any distribution lies between 0 and 1. Hence, plotting the CDF gives us a value less than equal to 1 which should be the range of ρ. However, if the channel is too good, there are chances that the value of ρ be tending to 1 thus, providing the entire received signal for RF EH. Thus, putting an upper limit seems suitable which is represented by Ψ here.

In (2), Ψ denotes the maximum value of ρ that can be allocated for EH at any given time-slot. SNR_i and SNR_{avg} denote instantaneous and average SNR, respectively. $Q_1(.,.)$ denotes the first-order Marcum Q function. As shown above, the value of ρ changes w.r.t the channel conditions. Dynamically setting the ρ factor, extracting more energy from RF signals when the channel conditions are favourable and lesser energy when it's not. Thus, the system is able to maintain a better relationship between EH and IT. However, optimality analysis is not included in the current work.

Algorithm 1 shows the procedure for calculating the harvested energy at R node. Here, we can select any $S_{i\in\{1,2,..,N\}}$, and receive the data transmitted by S_i in i^{th} time-slot and calculate SNR_i and SNR_{avg} from the signal received in that time-slot. Using (2), we calculate the value of ρ and store the harvested energy and power associated with it. Repeat the steps until all S_i transmits their data to R. Finally, R uses the harvested power to maintain a fixed relay power. Then R amplifies the combined data and broadcasts it using fixed relay power in $(N+1)^{th}$ time-slot.

[2]Assuming channels gains are constant during one frame of data transmission.

[3]Here we assume that the capacity of the battery for harvesting the energy is large enough.

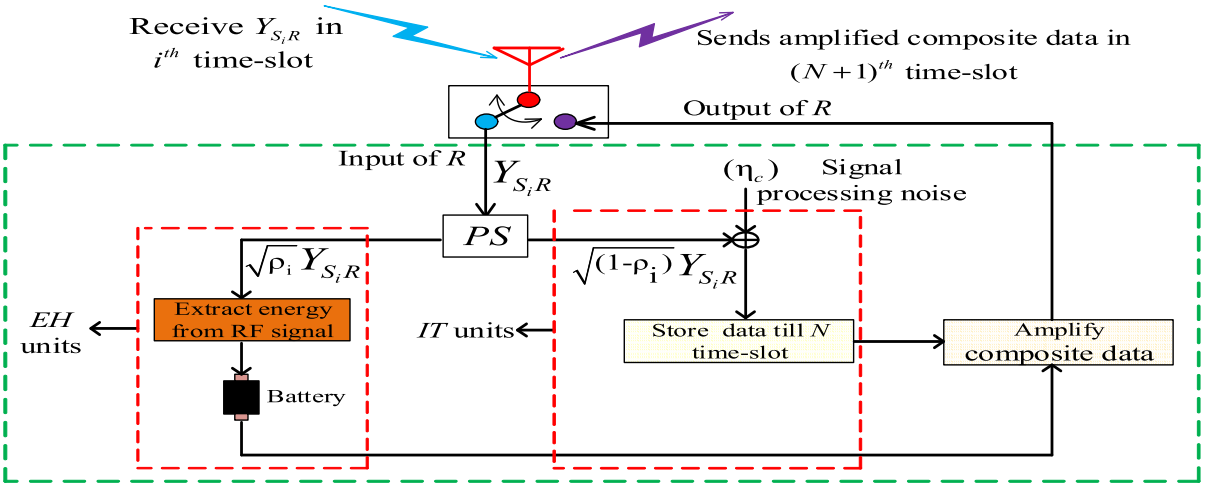

FIGURE 4. EH at relay node using PSR in DA-NCC for N $S-D$ pairs.

Algorithm 1: EH and It at R.

Set: $i = 1$.
while $N - i \neq 0$ **do**
  Receive the data from S_i in i^{th} time-slot.
  Calculate SNR_i from the signal received, $\mathcal{Y}_{S_iR}$.
  Initialize: Using (2), calculate the value of ρ.
  Perform EH and IT according to the calculated value of ρ and store energy and data.
  $i = i + 1$.
  Go to **Step 2.**
end
In the final time-slot, R uses the harvested power to maintain a fixed $\mathcal{P}_R$. Then R performs superposition coding on the stored data, amplifies it and transmits the data with power, $\mathcal{P}_R$.
Result: EH at R for prolonged life-time and aiding users by providing diversity.

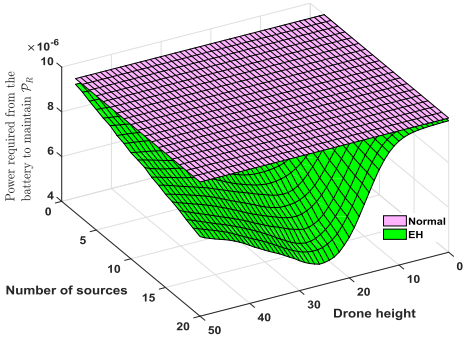

FIGURE 5. Power required from the battery of R w.r.t number of S_i and h_D.

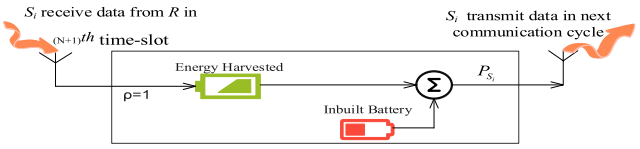

FIGURE 6. Block diagram for EH at $S_{i\in\{1,2,..,N\}}$ after $(N+1)^{th}$ time-slot.

Fig. 5 depicts the variation of battery used by R node w.r.t number of S_i and h_D. It can be seen in Fig. 5, as h_D increases, initially the amount of harvested power is more, thus, decreasing the amount of power extracted from the main battery of the R. This is due to the dominance of the LoS component over the path loss initially (around upto 25 m). On the other hand, a drastic decrease in power extraction from the main battery can be seen with increase in the number of participating S_i. This can be explained with the help of (26). As we can see in (26) that with increase in the number of sources, the harvested power increase and thus, decreasing the power extracted from the main battery. Although, as h_D increases (above 25 m), the path loss component starts to dominate over LoS component and the amount of power extracted from the main battery of the R increases. On the other hand, if power is not extracted (non EH case), a constant use of power from the main battery of the R is shown in Fig. 5. Here, it may also be noted that the harvested power at R improves the battery life of the R node.

3) ENERGY HARVESTING AT SOURCE NODE

In the system model of NCC in [3], signal from R is destined for D_i nodes only. However, it should be noted that due to broadcast nature of wireless channel, S_i nodes can also overhear this signal. By utilizing this observation, we propose the reception of signal from R by sources also and use it for the EH purpose. During $(N+1)^{th}$ time-slot, $S_{i\in\{1,2,..,N\}}$ nodes harvest energy from the signal coming from R. Fig. 6 shows the schematic of the proposed EH at S_i nodes. Since, there is no information extraction required at sources, received signal can be utilized completely for EH. Therefore, in this case $\rho = 1$, which means that the energy associated with signal is completely harvested at S_i nodes. During the transmission of the next packet by S_i, the harvested power can be utilized.

The power required from the battery is denoted by $\mathcal{P}'_{S_i}$ and defined as

$$\mathcal{P}'_{S_i} = \mathcal{P}_{S_i} - HP_S \tag{3}$$

where $\mathcal{P}_{S_i}$ denotes the power transmitted by S_i node and HP_S denotes the harvested power at S_i nodes.

Algorithm 2: Exchange of n Packets Along With EH for a Prolonged Transmitter Life.

1 Say, S_i has n packets to deliver to D_i.
2 **while** $n \neq 0$ **do**
3 **Set:** $\rho = 1$.
4 S_i wakes up at designated time-slot and transmits x_i in i^{th} time-slot.
5 **Set:** $n = n - 1$.
6 After transmission, S_i goes to sleep for another $N - i$ time-slots.
7 Wakes up at $(N+1)^{th}$ time-slot and R_x data broadcasted by R.
8 Harvest energy using the value of ρ.
9 Go to sleep for $i - 1$ time-slots.
10 **end**
Result: Successful operation of DA-NCC and EH at S_i along with prolonged life-time.

Algorithm 2 shows the procedure for calculating the harvested energy at S_i. Here, we assume that each S_i has n packets to transmit. Depending on the time-slot assigned during the set-up phase, each S_i transmits their data and goes into sleep mode. Within a communication cycle, S_i nodes wake-up and receive the signal broadcast by R in $(N+1)^{th}$ time-slot and harvest the energy by using (29).

B. PROBABILITY BASED STATISTICAL CHANNEL MODEL

In the proposed network, EH factor is a function of channel parameters/distribution. Therefore, it is imperative to model the channel accurately. Since, in a drone assisted networks, channel depends upon the drone height also, it is important to investigate the effect of drone height on channel as well as various system parameters. The $\mathbb{P}_L$ can be given as [5]

$$\mathbb{P}_L = \frac{1}{1 + ae^{ab}e^{-b\theta}} \tag{4}$$

where $\theta = \frac{180}{\pi}\tan^{-1}(\frac{h_D}{r_j})$, is the elevation angle between R and S_i (D_i) and a, b are constant values depending upon the environment [5]. $\mathbb{P}_{NL}$ may be found by using $\mathbb{P}_L + \mathbb{P}_{NL} = 1$. In order to make the model more realistic, this work takes the variation of Rician factor[4] by taking height into account using the following model [33]

$$M_{ij}(h_D, r_j) = A + (B - A)\frac{2\theta_{ij}}{\pi} \tag{5}$$

where M_{ij} denotes Rician factor between nodes i and j, A and B is in dB and θ_{ij} is in radian. The maximum value of M_{ij} approaches to B, if $\theta_{ij} \to \frac{\pi}{2}$ and minimum value of M_{ij} approaches to A, if $\theta_{ij} \to 0$. We also consider h_D dependent path loss exponent [33] for modelling large-scale attenuation defined as

$$\alpha = (\alpha_L - \alpha_{NL})\mathbb{P}_L + \alpha_{NL} \tag{6}$$

where α_L and α_{NL} are path loss exponents corresponding to $\mathbb{P}_L$ and $\mathbb{P}_{NL}$, respectively. By using the proposed channel model, the average received signal power at any node may be defined as

$$\bar{\mathcal{P}} = \mathbb{P}_L\mathcal{P}_{ij}^L + \mathbb{P}_{NL}\mathcal{P}_{ij}^{NL} \tag{7}$$

where $\mathcal{P}_{ij}^L$ and $\mathcal{P}_{ij}^{NL}$ denote the average received power corresponding to LoS and NLoS links when signal propagates from $i \in \{S, R\}$ to $j \in \{R, D\}$ node, respectively. Further, $\mathcal{P}_{ij}^L$ and $\mathcal{P}_{ij}^{NL}$ may be found by using the equations given below

$$\mathcal{P}_{ij}^L = \mathcal{P}_i d_{ij}^{-\alpha}|\hbar_{ij}^{\text{Ric}}|^2, \quad \mathcal{P}_{ij}^{NL} = \mathcal{P}_i d_{ij}^{-\alpha}|\hbar_{ij}^{\text{Ray}}|^2 \tag{8}$$

where $\mathcal{P}_i$, d_{ij}, $\hbar_{ij}$, Ric and Ray denote transmitted power by node i, distance between nodes i and j, channel coefficient between i and j nodes, Rician and Rayleigh fading, respectively.

Algorithm 3 is used for channel modelling in a DA-NCC scenario as shown in Fig. 2(a). The algorithm needs to be executed throughout one communication cycle for the network under consideration. The first N time-slots are needed at $S_{i\in\{1,2,..,N\}}$ (Algorithm 3: lines 1-11) and the last $(N+1)^{th}$ time-slot is required at R (Algorithm 3: lines 12-17) for completing the one communication cycle. For a given h_D and environmental parameters, $\mathbb{P}_{L_i}$ at S_i can be calculated by generating a uniformly distributed random number, g_i ($0 < g_i < 1$) and comparing it with $\mathbb{P}_{L_i}$. If it is less than $\mathbb{P}_{L_i}$, Rayleigh distribution is chosen. If not, Rician distribution is considered for the channel coefficient, $\hbar_{S_iR}$. Similarly, distribution of channel coefficient, $\hbar_{RD_i}$ can be found at R. It may be noted that within a communication cycle, all $N+1$ channels being statistically independent, follow two different distributions.

C. FRAME FORMAT FOR EVALUATING CSI AT RELAY AND DESTINATION NODES

It should be emphasized that the knowledge of the channel information/CSI towards undesired sources is also required in order to eliminate the undesired signals from the combined coded signal and extract the 2^{nd} copy of the desired signal. Depending on the initial network conditions/constraints, the process of delivering CSI to desired as well as other destinations can be obtained in various of ways. During set-up phase, users can transmit pilot signals in appropriate TDMA slots. For example, if a node, say $S_{i\in\{1,2,..,N\}}$, wants to communicate, it broadcasts a pilot signal to the entire network. Since all the network nodes are assumed to be at one hop distance, all D_i nodes (both desired and undesired) and R node can estimate the CSI between S_i and themselves using this pilot signal. During the decoding of signals at

[4]Height dependent Rician factor is also discussed in [19].

Algorithm 3: A2G Channel Allocation Based on $\mathbb{P}_L$.

Calculate $\mathbb{P}_L$ and $\mathbb{P}_{NL}$ for a given h_D and r_j at each $S_{i\in\{1,\ldots,N\}}$.
Set $i = 1$.
while $i \leq N$ **do**
  Generate random number, $g_{i\in\{1,\ldots,N\}}$ at each S_i for i^{th} time-slot.
  if $g_i < \mathbb{P}_L$ **then**
    Allocate $\hbar_{S_iR} \rightarrow$ Rician distributed.
  else
    Allocate $\hbar_{S_iR} \rightarrow$ Rayleigh distributed.
  end
  $i = i + 1$.
end
Generate random number, g_{N+1} at R for $(N+1)^{th}$ time-slot.
if $g_{N+1} < \mathbb{P}_L$ **then**
  Allocate $\hbar_{RD_i} \rightarrow$ Rician distributed.
else
  Allocate $\hbar_{RD_i} \rightarrow$ Rayleigh distributed.
end
Result: Allocation of channel distributions.

any destination, destinations subtract the overheard weighted signals which include all the channel coefficients ($\hbar_{S_iR}$, $\hbar_{RD_i}$ and $\hbar_{S_{j\neq i}D_i}$). Thus, the CSI of both $S_i - R$ and $R - D_i$ are required at the destinations. Now, the knowledge of channel between $R - D_i$ can be obtained at the destination by the exchange of pilot symbols between R-D_i. However, the knowledge of CSI between S_i and R cannot be obtained at destinations using pilot symbols. Hence, to make the CSI of S_i and R available at the destinations, we propose two different frame structures for the data and Acknowledgement (*ACK*) as shown in Fig. 7(a) and Fig. 7(b), respectively.

Normally in a multi-casting/broadcasting scenario, messages received are not acknowledged thus, raising questions on the QoS of a broadcasting scenario. To mend this problem, researches have been conducted and various schemes have been proposed. Authors in [34], propose a frame format where the nodes receiving the data only acknowledge it's reception if it is above a particular fixed target data rate. Although unlike [34], we design the data frame such that only the node whose address is succeeded by *ACK* Flag set to 1 acknowledges the data as shown in Fig. 7(a) where Rel_Add, Dest_Add and Tx_Add represent the relay address, destination address and transmit node address, respectively. Here, Rel_Add and Dest_Add are added in the address list and only *ACK* is asked from R because it is assumed that the data received at the destination is not reliable enough. Hence, asking for *ACK* from the respective destinations may supposed to decrease the throughput of the network without gaining much control information. Thus, on receiving data from source (say S_i), R acknowledges the reception by broadcasting an *ACK* frame. Before broadcasting, R adds

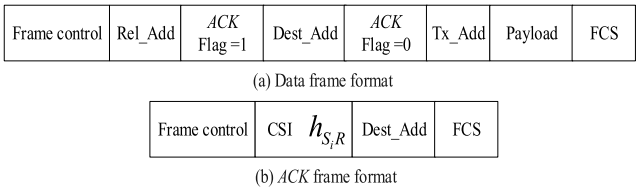

FIGURE 7. Frame structures for the proposed DA-NCC system, where FCS denotes frame check sequence.

the CSI of the channel between $S_i - R$ into *ACK* frame (shown in Fig. 7(b)) which is required at the destinations to decode the 2^{nd} copy of the desired data. This is received by both the source and destination nodes. The source nodes use this as an acknowledgement for the data sent whereas the destination nodes use it to obtain the CSI which is required while decoding the 2^{nd} copy of the required data.

IV. DESCRIPTION OF DA-NCC SYSTEM

This section includes the transmission-reception scheme, statistical parameters of ANC-noise and power allocation scheme at S_i and R node.

A. TRANSMISSION AND RECEPTION SCHEME FOR DA-NCC

In this subsection, we have developed the analytical framework for DA-NCC system. Consider $S_{i\in\{1,2,\ldots,N\}} - D_i$ pair as the pair of interest. In the 1^{st} N time-slots, S_i transmit their respective signals to D_i and R, which is overheard by $D_{j\neq i,j\in\{1,2,\ldots,N\}}$. The signals received by D_i, D_j and R can be modelled as

$$\begin{aligned}
\mathcal{Y}^{\text{Ray}}_{S_iD_i} &= \sqrt{\mathcal{P}_{S_i} d^{-\alpha}_{S_iD_i}}\,\hbar^{\text{Ray}}_{S_iD_i} x_i + \eta_{S_iD_i} \\
\mathcal{Y}^{l_i}_{S_iR} &= \sqrt{\mathcal{P}_{S_i} d^{-\alpha}_{S_iR}}\,\hbar^{l_i}_{S_iR} x_i + \eta_{S_iR}, \text{ and} \\
\mathcal{Y}^{\text{Ray}}_{S_iD_j} &= \sqrt{\mathcal{P}_{S_i} d^{-\alpha}_{S_iD_j}}\,\hbar^{\text{Ray}}_{S_iD_j} x_i + \eta_{S_iD_j}
\end{aligned} \tag{9}$$

where $l_{i\in\{1,2,..,N\}} \in \{\text{Ray}, \text{Ric}\}$. The above equations include transmitted power by S_i ($\mathcal{P}_{S_i}$), large-scale attenuation ($d^{-\alpha}_{mn}$) and small scale ($\hbar_{mn}$) fading. It also includes d_{mn}, α and $\hbar_{mn}$ which denote distance between m and n nodes, path loss exponent and channel coefficient between nodes m and n, respectively. The Additive White Gaussian Noise (AWGN) between node m and n is denoted by η_{mn} with $\mathcal{N} \in \{0, \sigma^2\}$. The signals received at the input of energy-harvester in the 1^{st} N time-slots are expressed as

$$\mathcal{Y}^{EH_i,l_i}_{S_iR} = \sqrt{\rho_i}\mathcal{Y}^{l_i}_{S_iR} = \sqrt{\rho_i \mathcal{P}_{S_i} d^{-\alpha}_{S_iR}}\,\hbar^{l_i}_{S_iR} x_i + \sqrt{\rho_i}\eta_{S_iR} \tag{10}$$

and IT received at R in the 1^{st} N time-slots is written as

$$\begin{aligned}
\mathcal{Y}^{IT_i,l_i}_{S_iR} &= \sqrt{(1-\rho_i)}\mathcal{Y}^{l_i}_{S_iR} + \eta_c \\
&= \sqrt{(1-\rho_i)\mathcal{P}_{S_i} d^{-\alpha}_{S_iR}}\,\hbar^{l_i}_{S_iR} x_i + \eta_{R_i}
\end{aligned} \tag{11}$$

where $\eta_{R_i} = \sqrt{(1-\rho_i)}\eta_{S_iR} + \eta_c$ having zero mean and variance, $\sigma^2_{R_i} = (1-\rho_i)\sigma^2_{S_iR} + \sigma^2_c$. R combines $x_{i,i\in\{1,2,\ldots,N\}}$,

amplifies and broadcasts the coded signal in $(N+1)^{th}$ time-slot. The signal received at D_i in $(N+1)^{th}$ time-slot can be represented as

$$\mathcal{Y}_{RD_i}^{l_{N+1}} = \mathbb{Q}^{l_1,l_2,..,l_N} x_R(\sqrt{d_{RD_i}^{-\alpha}}\hbar_{RD_i}^{l_{N+1}}) + \eta_{RD_i}. \tag{12}$$

where $l_{N+1} \in \{\text{Ray, Ric}\}$ and x_R denotes ANC signal, given as

$$x_R = \sum_{i=1}^{N} \mathcal{Y}_{S_iR}^{IT_i,l_i} \tag{13}$$

and $\mathbb{Q}$ is known as amplification factor given as [3]

$$\mathbb{Q}^{l_1,l_2,..,l_N} = \sqrt{\frac{\mathcal{P}_R}{\sum_{i=1}^{N}\left[(1-\rho_i)\mathcal{P}_{S_i} d_{S_iR}^{-\alpha}\left|\hbar_{S_iR}^{l_i}\right|^2 + \sigma_{R_i}^2\right]}}. \tag{14}$$

By using (9), (12) and (13), node D_i can get the 2^{nd} copy of desired signal as follows

$$\hat{\mathcal{Y}}_{RD_i}^{l_{N+1}} = \mathbb{Q}^{l_1,l_2,..,l_N}\sqrt{d_{RD_i}^{-\alpha}}\hbar_{RD_i}^{l_i}\mathcal{Y}_{S_iR}^{IT_i,l_i} + \mathcal{N}_i^{l_{N+1}} \tag{15}$$

where $\mathcal{N}_i$ denotes ANC-noise component at D_i. The ANC-noise at D_i comes during the subtraction of $\sum_{j=1,j\neq i}^{N}\mathcal{Y}_{S_jRD_i}$ with $\sum_{j=1,j\neq i}^{N}\mathcal{Y}_{S_jD_i}$. This process results in the residual term $(\sum_{j=1,j\neq i}^{N}(\mathcal{Y}_{S_jRD_i} - \mathcal{Y}_{S_jD_i}))$ due to asymmetric channel characteristics of direct path and path via relay between S_j and D_i, power allocation factor and path length. The ANC-noise component at D_i given in (16)

$$\begin{aligned}\mathcal{N}_i^{l_1,l_2,..,l_N,l_{N+1}} &= \eta_{RD_i} + \sum_{j=1,j\neq i}^{N}\mathbb{Q}^{l_1,l_2,..,l_N}\sqrt{d_{RD_i}^{-\alpha}}\hbar_{RD_i}^{l_{N+1}}\eta_{R_j} \\ &- \sum_{j=1,j\neq i}^{N}\mathbb{Q}^{l_1,l_2,..,l_N}\left(\frac{\sqrt{(1-\rho_j)d_{RD_i}^{-\alpha}d_{S_jR}^{-\alpha}}}{\sqrt{d_{S_jD_i}^{-\alpha}}}\right) \\ &\times\left(\frac{\hbar_{RD_i}^{l_{N+1}}\hbar_{S_jR}^{l_j}}{\hbar_{S_jD_i}^{\text{Ray}}}\right)\eta_{S_jD_i}.\end{aligned} \tag{16}$$

where $\eta_{R_j} = \sqrt{(1-\rho_i)}\eta_{S_jR} + \eta_c$ having mean zero and variance $\sigma_{R_j}^2 = (1-\rho_i)\sigma_{S_jR}^2 + \sigma_c^2$.

B. STATISTICAL PARAMETERS OF ANC-NOISE

In this sub-section, we derive the statistical parameters such as mean and variance of ANC-noise.

1) MEAN

For a given drone height, the mean of (16) is zero because the background noise at node D_i and R are statistically independent with zero mean ($\mathrm{E}[\eta_{D_i}] = \mathrm{E}[\eta_{R_j}] = 0$).

2) VARIANCE

The variance of ANC-noise component at node D_i for a given h_D, is defined as

$$\begin{aligned}&var(\mathcal{N}_i^{l_1,l_2,..,l_N,l_{N+1}}) \\ &= var(\eta_{RD_i} + \sum_{j=1,j\neq i}^{N}\mathbb{Q}^{l_1,l_2,..,l_N}\sqrt{d_{RD_i}^{-\alpha}}\hbar_{RD_i}^{l_{N+1}}\eta_{R_j} \\ &- \sum_{j=1,j\neq i}^{N}\mathbb{Q}^{l_1,l_2,..,l_N}\left(\frac{\sqrt{(1-\rho_j)d_{RD_i}^{-\alpha}d_{S_jR}^{-\alpha}}}{\sqrt{d_{S_jD_i}^{-\alpha}}}\right) \\ &\times\left(\frac{\hbar_{RD_i}^{l_{N+1}}\hbar_{S_jR}^{l_j}}{\hbar_{S_jD_i}^{\text{Ray}}}\right)\eta_{S_jD_i}).\end{aligned} \tag{17}$$

where **var** denotes variance of $\mathcal{N}_i^{l_1,l_2,..,l_N,l_{N+1}}$ given as

$$\begin{aligned}&\sigma^2_{\mathcal{N}_i^{l_1,l_2,..,l_N,l_{N+1}}} \\ &= var(\eta_{RD_i} + \sum_{j=1,j\neq i}^{N}\mathbb{Q}^{l_1,l_2,..,l_N}\sqrt{d_{RD_i}^{-\alpha}}\hbar_{RD_i}^{l_{N+1}}\eta_{R_j} \\ &- \sum_{j=1,j\neq i}^{N}\mathbb{Q}^{l_1,l_2,..,l_N}\left(\frac{\sqrt{(1-\rho_j)d_{RD_i}^{-\alpha}d_{S_jR}^{-\alpha}}}{\sqrt{d_{S_jD_i}^{-\alpha}}}\right) \\ &\times\left(\frac{\hbar_{RD_i}^{l_{N+1}}\hbar_{S_jR}^{l_j}}{\hbar_{S_jD_i}^{\text{Ray}}}\right)\eta_{S_jD_i}).\end{aligned} \tag{18}$$

Since, η_{RD_i}, η_{R_j} and $\eta_{S_jD_i}$ are assumed to be independent of each other, above equation can be written as

$$\begin{aligned}&\sigma^2_{\mathcal{N}_i^{l_1,l_2,..,l_N,l_{N+1}}} \\ &= var(\eta_{RD_i}) + var(\sum_{j=1,j\neq i}^{N}\mathbb{Q}^{l_1,l_2,..,l_N}\sqrt{d_{RD_i}^{-\alpha}}\hbar_{RD_i}^{l_{N+1}}\eta_{R_j}) \\ &- var(\sum_{j=1,j\neq i}^{N}\mathbb{Q}^{l_1,l_2,..,l_N}\left(\frac{\sqrt{(1-\rho_j)d_{RD_i}^{-\alpha}d_{S_jR}^{-\alpha}}}{\sqrt{d_{S_jD_i}^{-\alpha}}}\right) \\ &\times\left(\frac{\hbar_{RD_i}^{l_{N+1}}\hbar_{S_jR}^{l_j}}{\hbar_{S_jD_i}^{\text{Ray}}}\right)\eta_{S_jD_i}).\end{aligned} \tag{19}$$

Using the property of the variance and the fact that $\mathbb{Q}^{l_1,l_2,..,l_N}$, $\hbar_{RD_i}^{l_{N+1}}$, $\hbar_{S_jR}^{l_j}$ and $\hbar_{S_jD_i}^{\text{Ray}}$ are assumed to be constant for a packet duration, above equation can be written as

$$\begin{aligned}&\sigma^2_{\mathcal{N}_i^{l_1,l_2,..,l_N,l_{N+1}}} \\ &= var(\eta_{RD_i}) + (\sum_{j=1,j\neq i}^{N}\mathbb{Q}^{l_1,l_2,..,l_N}\sqrt{d_{RD_i}^{-\alpha}}\hbar_{RD_i}^{l_{N+1}})^2 var(\eta_{R_j}) \\ &-(\sum_{j=1,j\neq i}^{N}\mathbb{Q}^{l_1,l_2,..,l_N}\left(\frac{\sqrt{(1-\rho_j)d_{RD_i}^{-\alpha}d_{S_jR}^{-\alpha}}}{\sqrt{d_{S_jD_i}^{-\alpha}}}\right) \\ &\times\left(\frac{\hbar_{RD_i}^{l_{N+1}}\hbar_{S_jR}^{l_j}}{\hbar_{S_jD_i}^{\text{Ray}}}\right))^2 var(\eta_{S_jD_i}).\end{aligned} \tag{20}$$

Finally the variance of ANC-noise component at node D_i for a given h_D, is given as

$$\sigma^2_{\mathcal{N}_i^{l_1,l_2,..,l_N,l_{N+1}}} = \Big[\sigma^2_{RD_i} + \mathbb{Q}^{l_1,l_2,..,l_N}\Big(\sum_{j=1,j\neq i}^{N}(\sqrt{d^{-\alpha}_{RD_i}}\hbar^{l_{N+1}}_{RD_i})^2\sigma^2_{R_j} + \sum_{j=1,j\neq i}^{N}\left(\left(\frac{\sqrt{(1-\rho_j)d^{-\alpha}_{RD_i}d^{-\alpha}_{S_jR}}}{\sqrt{d^{-\alpha}_{S_jD_i}}}\right)\left(\frac{\hbar^{l_{N+1}}_{RD_i}\hbar^{l_j}_{S_jR}}{\hbar^{\text{Ray}}_{S_jD_i}}\right)\right)^2 \times \sigma^2_{S_jD_i}\Big)\Big]. \quad (21)$$

From (21), it is clear that the variance of ANC-noise increases as number of $S-D$ pair increases.

3) ANC-NOISE FOR STATISTICAL CHANNEL MODEL

For a given N number of $S-D$ pairs, the effective values of $\mathcal{N}_i^{l_1,l_2,..,l_N,l_{N+1}}$ and $\sigma^2_{\mathcal{N}_i^{l_1,l_2,..,l_N,l_{N+1}}}$ for ANC-noise in case of statistical channel model can be found by averaging (16) and (21) over all the $N+1$ possible cases (as discussed in Sec.V) of various combinations of $l_1, l_2, .., l_N, l_{N+1}$ as:

$$\mathcal{N}_i^{avg} = \sum_{j=1}^{2^{(N+1)}}\left[\left(\prod_{l=1}^{N+1}\mathbb{P}_{m_l}\right)\mathcal{N}_i^{l_1,l_2,...,l_{N+1}}\right]_j \quad (22)$$

$$\sigma^2_{\mathcal{N}_i^{avg}} = \sum_{j=1}^{2^{(N+1)}}\left[\left(\prod_{l=1}^{N+1}\mathbb{P}_{m_l}\right)\sigma^2_{\mathcal{N}_i^{l_1,l_2,...,l_{N+1}}}\right]_j \quad (23)$$

where $m_1, m_2, \ldots, m_{N+1} \in \{L, NL\}$ and $l_1, l_2, \ldots, l_{N+1} \in \{\text{Ray}, \text{Ric}\}$. Here, L and NL correspond to Ric and Ray channel, respectively.

C. DIFFERENT POWER ALLOCATION SCHEMES AT RELAY AND SOURCES

In this sub-section, we discuss the power allocation scheme for different S_i and R. The power allocated to S_i and R nodes are denoted by $\mathcal{P}_{S_i}$ and $\mathcal{P}_R$, respectively.

1) EH AT RELAY NODE

The EH at R can be written as

$$E^{l_i}_{H_i} = \frac{\eta\rho_i\mathcal{P}_{S_i}d^{-\alpha}_{S_iR}|\hbar^{l_i}_{S_iR}|^2T}{N+1} \quad (24)$$

where $0 < \eta \leq 1$ is the EH efficiency determined mainly by the circuitry [21]. The harvested energy at R after N time-slots is written as

$$E_H = \sum_{i=1}^{N}E^{l_i}_{H_i}. \quad (25)$$

Similarly the harvested power at R after N time-slots can be obtained as

$$\mathcal{P}'_R = \frac{E_H}{\left(\frac{T}{N+1}\right)}, \quad \mathcal{P}'_R = \sum_{i=1}^{N}\eta\rho_i\mathcal{P}_{S_i}d^{-\alpha}_{S_iR}|\hbar^{l_i}_{S_iR}|^2 \quad (26)$$

where $0 \leq \rho_i \leq 1$. The effective value of $\mathcal{P}'_R$ for statistical channel model is given as

$$\mathcal{P}'^{\text{avg}}_R = \sum_{i=1}^{N}[\mathbb{P}_{NL}(\eta\rho_i\mathcal{P}_{S_i}d^{-\alpha}_{S_iR}|\hbar^{\text{Ray}}_{S_iR}|^2) + \mathbb{P}_L(\eta\rho_i\mathcal{P}_{S_i}d^{-\alpha}_{S_iR}|\hbar^{\text{Ric}}_{S_iR}|^2)]. \quad (27)$$

During the transmission of the coded packet (formed by combining data sent by different sources) in $(N+1)^{th}$ time-slot, the power required from the battery to transmit that packet at fixed power ($\mathcal{P}_R$) is defined as

$$\mathcal{P}''_R = \mathcal{P}_R - \mathcal{P}'^{\text{avg}}_R. \quad (28)$$

2) EH AT SOURCE NODES

Within a communication cycle, the harvested power at each S_i is denoted by HP_S and defined as

$$HP_S = (\mathbb{Q}^{l_1,l_2,..,l_N}\sqrt{d^{-\alpha}_{RD_i}}\hbar^{l_{N+1}}_{RS_i})^2\sum_{i=1}^{N}\eta(1-\rho_i)\mathcal{P}_{S_i}d^{-\alpha}_{S_iR}|\hbar^{l_i}_{S_iR}|^2. \quad (29)$$

Similarly the effective value of harvested power at each S_i is calculated as[5]

$$HP^{\text{avg}}_S = [\sqrt{d^{-\alpha}_{RD_i}}(\mathbb{P}_{NL}(\mathbb{Q}^{l_1,l_2,..,l_N}\hbar^{\text{Ray}}_{RS_i})^2 + \mathbb{P}_L(\mathbb{Q}^{l_1,l_2,..,l_N}\hbar^{\text{Ric}}_{RS_i})^2)] \times \sum_{i=1}^{N}[\mathbb{P}_{NL}(\eta(1-\rho_i)\mathcal{P}_{S_i}d^{-\alpha}_{S_iR}|\hbar^{\text{Ray}}_{S_iR}|^2) + \mathbb{P}_L(\eta(1-\rho_i)\mathcal{P}_{S_i}d^{-\alpha}_{S_iR}|\hbar^{\text{Ric}}_{S_iR}|^2)]. \quad (30)$$

During the transmission of the $i^{th}(i \in \{2, 3, .., n\})$ packet, the power required from the battery to transmit the packet at fixed power ($\mathcal{P}_{S_i}$) is defined as

$$\mathcal{P}'_{S_i} = \mathcal{P}_{S_i} - \sum_{j=1}^{i-1}j(HP^{\text{avg}}_S). \quad (31)$$

Fig. 8 shows the variation of WPS factor (1), Y_1 and power associated with IT (11), Y_2 at drone w.r.t h_D. The reason for the curves having different slopes for Y_1 and Y_2 may again be explained as done before for Fig. 5. Here, we observed that for lower values of h_D (below $h_{D_{opt}} \approx 12$ m), the values of ρ decreases and power associated with IT increases. For higher values of h_D (above $h_{D_{opt}}$), the values of ρ increases and power associated with IT decreases.

Fig. 9 shows the variation of harvested power at S_i w.r.t h_D. Now, as discussed earlier, as the drone height starts increasing, there is a higher probability of LoS between the sources and relay. Thus, there is an increased probability of Rician fading which helps the sources to harvest more power. This can be observed in the figure as the graph shows an

[5]It can be argued that EH can be applied at the destination nodes. It has not been considered in this case, because the data being transmitted by R is required by the destination nodes during the extraction of the 2^{nd} copy of the desired signal, whereas the source nodes do not require it.

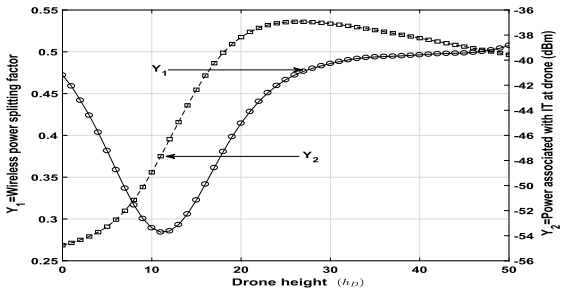

FIGURE 8. WPS factor and power associated with IT at R w.r.t h_D (meter).

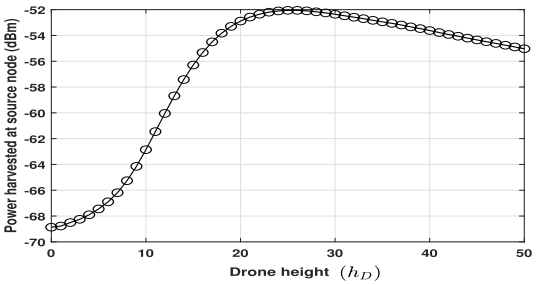

FIGURE 9. Power harvested at S_i node w.r.t h_D (meter).

increasing nature. However, the average harvested power falls after a certain drone height ($h_{D_{opt}} \approx 25$ m). This is because after a certain value of $h_{D_{opt}}$ the distance becomes so large that eventually the gain cause due to LoS component takes a back seat and it is overpowered by the path loss component. Here, it may also be noted that the harvested power at S_i improves the battery life of the S_i nodes.

V. RATE AND OUTAGE ANALYSIS FOR DA-NCC

Here, we formulate the analytical expressions of the rate and outage probability for DA-NCC system using EH at R and S_i.

A. RATE ANALYSIS

As shown in Fig. 2(a), the time required to complete the one communication cycle is T and $\frac{\mathrm{T}}{N+1}$ is the time-slot assigned to each S_i and R. For N $S-D$ pairs, the rate at node D_i is defined as

$$\mathbb{C}_{\text{DA-NCC}}^{l_1,l_2,..,l_N,l_{N+1}} = \left(\frac{1}{N+1}\right)\mathbb{I}_{\text{DA-NCC}}^{l_1,l_2,..,l_N,l_{N+1}} \tag{32}$$

where $\mathbb{I}_{\text{DA-NCC}}^{l_1,l_2,..,l_N,l_{N+1}}$ denotes mutual information at node D_i. The mutual information at D_i is calculated by using MRC technique, where we combine the direct path ($S_i - D_i$) and the relay path ($S_i - R - D_i$) SNRs, which is defined as [3]

$$\mathbb{I}_{\text{DA-NCC}}^{l_1,l_2,..,l_N,l_{N+1}} = \log_2[1 + (\Upsilon_{S_iD_i}^{\text{Ray}} + \Upsilon_{S_iRD_i}^{l_1,l_2,..,l_N,l_{N+1}})]. \tag{33}$$

In (33), the SNR between node $\mathfrak{a}$ and $\mathfrak{b}$ is denoted by $\Upsilon_{\mathfrak{a}\mathfrak{b}}$ and found by using

$$\Upsilon_{\mathfrak{a}\mathfrak{b}}^{l_i} = \frac{\mathcal{P}_{\mathfrak{a}} d_{\mathfrak{a}\mathfrak{b}}^{-\alpha} |\hbar_{\mathfrak{a}\mathfrak{b}}^{l_i}|^2}{\sigma_{\mathfrak{b}}^2} \tag{34}$$

and symbol $\Upsilon_{S_iRD_i}^{l_1,l_2,..,l_N,l_{N+1}}$ represents SNR at node D_i via relay path. Substituting (11) into (15), we can define $\Upsilon_{S_iRD_i}^{l_1,l_2,..,l_N,l_{N+1}}$ as in (35), shown at the top of the next page. After performing few mathematical simplification in (36), shown at the top of the next page we can get (37), shown at the top of the next page. In (37), $\Upsilon_{\mathfrak{a}\mathfrak{b}}$ can be found by using (34), where $\mathfrak{a} \in \{S_{i,i\in\{1,2,..,N\}}, R\}$ and $\mathfrak{b} \in \{R, D_{i,i\in\{1,2,...,N\}}\}$.

B. OUTAGE ANALYSIS

In this subsection, we investigate the generalized expression of the outage probability for N number of $S_{i\in\{1,2...,N\}} - D_i$ pairs by using MRC scheme at the desired node (D_i). Among all the N number of $S_i - D_i$ pairs, D_i is considered as the node of interest.

For a given spectral efficiency ($\mathcal{R}$), the outage probability is defined as [5]

$$\mathbb{P}_{\text{out}}^{l_1,l_2,..,l_N,l_{N+1}} = \mathbb{P}\left[\left(\frac{1}{N+1}\right)\mathbb{I}_{\text{DA-NCC}}^{l_1,l_2,..,l_N,l_{N+1}}(D_i) < \mathcal{R}\right]. \tag{38}$$

Using (33) and (38), outage probability for DA-NCC becomes

$$\mathbb{P}_{\text{out}}^{l_1,l_2,..,l_N,l_{N+1}} = \mathbb{P}\left[(\Upsilon_{S_iD_i}^{\text{Ray}} + \Upsilon_{S_iRD_i}^{l_1,l_2,..,l_N,l_{N+1}}) < T_N\right] \tag{39}$$

where $T_N = (2^{(N+1)\mathcal{R}} - 1)$. Channels among GUs and drone are modelled using the probability based statistical approach. By taking the possible values of l_i, l_j and l_{N+1} into account, there are 2^{N+1} possible cases of the outage probability for the proposed channel model explained as:

1) CASE I

Out of the 2^{N+1} cases, one possible instance occurs when S_i to R, S_j to R and R to D_i links are Rayleigh faded. Probability of occurrence of this case is given by $\prod_{i=1}^{N}[P_{NL}]_i$. Putting l_i = Ray, l_j = Ray, Ray,.., $N-1$ times and l_{N+1} = Ray in (39) and rewritten (39) as

$$\mathbb{P}_{\text{out}}^{\text{Ray; Ray,...,Ray; Ray}} = \mathbb{P}\left[(\Upsilon_{S_iD_i}^{\text{Ray}} + \Upsilon_{S_iRD_i}^{\text{Ray; Ray,...,Ray; Ray}}) < T_N\right]. \tag{40}$$

2) CASE II

Another possibility is that the S_i to R, S_j to R, links are Rayleigh faded and the R to D_i link is Rician faded. Probability of occurrence of this possibility can be calculated by $\prod_{i=1}^{N}[P_{NL}]_i P_L$. Putting l_i = Ray, l_j = Ray, Ray,.., $N-1$ times and l_{N+1} = Ric in (39) and rewritten (39) as given below

$$\mathbb{P}_{\text{out}}^{\text{Ray; Ray,...,Ray; Ric}} = \mathbb{P}\left[(\Upsilon_{S_iD_i}^{\text{Ray}} + \Upsilon_{S_iRD_i}^{\text{Ray; Ray,...,Ray; Ric}}) < T_N\right]. \tag{41}$$

3) CASE $2^{N+1}-1$

The $(2^{N+1}-1)^{th}$ instance occurs when the links S_i to R, S_j to R are Rician faded and the link R to D_i is Rayleigh faded, respectively. Probability of occurrence of this possibility can be calculated by $\prod_{i=1}^{N}[P_L]_i P_{NL}$. Putting l_i = Ric, l_j = Ric,

$$\gamma_{S_iRD_i}^{l_1,l_2,..,l_N,l_{N+1}} = \frac{(\mathbb{Q}^{l_1,l_2,..,l_N})^2 d_{RD_i}^{-\alpha} |\hbar_{RD_i}^{l_{N+1}}|^2 (1-\rho_i)\mathcal{P}_{S_i} d_{S_iR}^{-\alpha} |\hbar_{S_iR}^{l_i}|^2}{(\mathbb{Q}^{l_1,l_2,..,l_N})^2 d_{RD_i}^{-\alpha} |\hbar_{RD_i}^{l_{N+1}}|^2 \sigma_{R_i}^2 + \sigma^2_{\mathcal{N}_i^{l_1,l_2,...,l_N,l_{N+1}}}}. \tag{35}$$

Putting the value of $\mathbb{Q}^{l_1,l_2,...,l_N}$ from (14) into (35), we can rewrite (35) as

$$\gamma_{S_iRD_i}^{l_1,l_2,..,l_N,l_{N+1}} = \frac{\mathcal{P}_R d_{RD_i}^{-\alpha} |\hbar_{RD_i}^{l_{N+1}}|^2 (1-\rho_i)\mathcal{P}_{S_i} d_{S_iR}^{-\alpha} |\hbar_{S_iR}^{l_i}|^2}{\mathcal{P}_R d_{RD_i}^{-\alpha} |\hbar_{RD_i}^{l_{N+1}}|^2 \sigma_{R_i}^2 + \sigma^2_{\mathcal{N}_i^{l_1,l_2,...,l_N,l_{N+1}}} \sum_{i=1}^{N} \left[(1-\rho_i)\mathcal{P}_{S_i} d_{S_iR}^{-\alpha} \left|\hbar_{S_iR}^{l_i}\right|^2 + \sigma_{R_i}^2 \right]}. \tag{36}$$

$$\gamma_{S_iRD_i}^{l_1,l_2,..,l_N,l_{N+1}} = \frac{\left(\frac{(1-\rho_i)\gamma_{RD_i}^{l_{N+1}} \gamma_{S_iR}^{l_i}}{\prod_{j=1,j\neq i}^{N} \sigma_{R_j}^2} \right)}{\left(\frac{\gamma_{RD_i}^{l_{N+1}}}{\prod_{j=1,j\neq i}^{N} \sigma_{R_j}^2} \right) + \frac{\sigma^2_{\mathcal{N}_i}}{\sigma^2_{D_i}} \left(\sum_{i=1}^{N} \left(\frac{(1-\rho_i)\gamma_{S_iR}^{l_i}}{\prod_{j=1,j\neq i}^{N} \sigma_{R_j}^2} \right) + \sum_{i=1}^{N} \left(\frac{\sigma_{R_i}^2}{\prod_{i=1}^{N} \sigma_{R_i}^2} \right) \right)}. \tag{37}$$

Ric,.., N-1 times and l_{N+1} = Ray in (39) and rewritten (39) as

$$\mathbb{P}_{\text{out}}^{\text{Ric; Ric,...,Ric; Ray}} = \mathbb{P}\left[(\gamma_{S_iD_i}^{\text{Ray}} + \gamma_{S_iRD_i}^{\text{Ric; Ric,...,Ric; Ray}}) < T_N \right]. \tag{42}$$

4) CASE 2^{N+1}

The $(2^{N+1})^{th}$ instance occurs when S_i to R, S_j to R and R to D_i links are Rician faded, respectively. Probability of occurrence of this case can be calculated by $\prod_{i=1}^{N} [P_L]_i$. Putting l_i = Ric, l_j = Ric, Ric,.., $N-1$ times and l_{N+1} = Ric in (39) and rewritten (39) as

$$\mathbb{P}_{\text{out}}^{\text{Ric; Ric,...,Ric; Ric}} = \mathbb{P}\left[(\gamma_{S_iD_i}^{\text{Ray}} + \gamma_{S_iRD_i}^{\text{Ric; Ric,...,Ric; Ric}}) < T_N \right]. \tag{43}$$

$\mathbb{P}_{\text{out}}$ for cases III, IV,..., $2^{N+1}-2$ may be calculated in the same way as discussed above by taking different possible values of l_i, l_j and l_{N+1}. By including all the cases depending upon $\mathbb{P}_L$ and $\mathbb{P}_{NL}$, the average rate and the average outage probability for N number of $S-D$ pairs using the probabilistic channel model can be found in (44) and (45) as written below

$$\mathbb{C}_{\text{rate}}^{\text{avg}} = \sum_{i=1}^{2^{N+1}} \left[\left(\prod_{j=1}^{N+1} \mathbb{P}_{m_j} \right) \mathbb{C}_{\text{rate}}^{l_1,l_2,...,l_{N+1}} \right]_i \tag{44}$$

$$\mathbb{P}_{\text{out}}^{\text{avg}} = \sum_{i=1}^{2^{N+1}} \left[\left(\prod_{j=1}^{N+1} \mathbb{P}_{m_j} \right) \mathbb{P}_{\text{out}}^{l_1,l_2,...,l_{N+1}} \right]_i \tag{45}$$

Final expression for the average $\mathbb{C}_{\text{rate}}$ and average $\mathbb{P}_{\text{out}}$ are obtained by weighing each case with corresponding probability of occurrence. The average capacity (44) and outage (45) expressions derived, provide useful insights to the system engineers for evaluating the system performance such as spectral efficiency in Internet of Things (IoT) based smart agriculture scenario where asymmetric object distribution in the environment leads to dissimilar fading among various GUs and hence, justifies the application of the proposed probability based channel assignment model.

TABLE 2. Simulation parameters.

Parameter	Value
Number of sources (N)	2-20
Power allocated to sources ($\mathcal{P}_{S_i}$)	0-10 dBm
Power allocated to Relay ($\mathcal{P}_R$)	-20 dBm
Noise power	-70 dBm
α_L, α_{NL}	2, 3.5
Urban environment	a=9.61, b=0.16
Fading type	Rayleigh, Rician
Vertical height (h_D)	0:100 m
A and B	1 and 10 dB
$d_{S_1D_1}, d_{S_1D_2}, d_{S_2D_1}, d_{S_2D_2}$	50 m
Spectral efficiency ($\mathcal{R}$)	-2dB to 2dB

VI. SIMULATION RESULTS

In this section, various results are presented to validate the proposed analytical framework. Algorithm 4 is used during the calculation of the average outage probability and average capacity through simulations for N number of $S-D$ pairs. For a given h_D and environmental parameters, $\mathbb{P}_{L_i}$ at S_i can be calculated as mentioned in algorithm 4.

For this purpose, generate a uniformly distributed random number g_i and compare it with $\mathbb{P}_{L_i}$. If g_i is less than $\mathbb{P}_{L_i}$, choose Rayleigh distribution else Rician distribution for the channel coefficient $\hbar_{S_iR}$. Again, using the similar steps at R also, distribution of the channel coefficient $\hbar_{RD_i}$ can be found. Now calculate $\mathbb{I}_{\text{rate}}^{l_1,l_2,l_3,...,l_{N+1}}$ and $\mathbb{P}_{\text{out}}^{l_1,l_2,l_3,...,l_{N+1}}$ using (32) and (39) respectively, in each communication cycle. In the last

Algorithm 4: Evaluation of $\mathbb{P}_{\text{out}}$ and $\mathbb{C}_{\text{rate}}$ for N $S-D$ Pairs.

iteration = 1:J; χ = length (h_D);
for i = 1 $\rightarrow$ χ **do**
  $\text{count}_1 = 0; \text{count}_2 = 0; \ldots; \text{count}_{2^{N+1}} = 0;$
  for j = 1 $\rightarrow$ length (iteration) **do**
    Calculate $\mathbb{P}_L$ and $\mathbb{P}_{NL}$ for given h_D and r_j
    Generate a random number $g_{i\in\{1,2,3,\ldots,N\}}$ at S_i and g_{N+1} at R
    if $g_1 < \mathbb{P}_L, g_2 < \mathbb{P}_L, \ldots, g_{N+1} < \mathbb{P}_L$ **then**
      $\hbar_{S_1R}, \hbar_{S_2R}, \ldots, \hbar_{S_NR}$ and $\hbar_{RD_i} \rightarrow$ Rician distributed
      Calculate $\mathbb{C}_{\text{rate}}^{\text{Ric, Ric,Ric,}\ldots\text{,Ric}}$ & $\mathbb{P}_{\text{out}}^{\text{Ric, Ric,Ric,}\ldots\text{,Ric}}$, using (32) & (39)
      $\text{count}_1 = \text{count}_1 + 1;$
    else
      $\mathbb{C}_{\text{rate}}^{\text{Ric, Ric,Ric,}\ldots\text{,Ric}} = 0, \mathbb{P}_{\text{out}}^{\text{Ric, Ric,Ric,}\ldots\text{,Ric}} = 0$
    end if
      $\vdots \quad \vdots \quad \vdots$
    if $g_1 > \mathbb{P}_L, g_2 > \mathbb{P}_L, \ldots, g_{N+1} > \mathbb{P}_L$ **then**
      $\hbar_{S_1R}, \hbar_{S_2R}, \ldots, \hbar_{S_NR}$ and $\hbar_{RD_i} \rightarrow$ Rayleigh distributed
      Calculate $\mathbb{C}_{\text{rate}}^{\text{Ray, Ray,Ray,}\ldots\text{,Ray}}$ & $\mathbb{P}_{\text{out}}^{\text{Ray, Ray,Ray,}\ldots\text{,Ray}}$, using (32) & (39)
      $\text{count}_{(2^{N+1})} = \text{count}_{(2^{N+1})} + 1;$
    else
      $\mathbb{C}_{\text{rate}}^{\text{Ray, Ray,Ray,}\ldots\text{,Ray}} = 0, \mathbb{P}_{\text{out}}^{\text{Ray, Ray,Ray,}\ldots\text{,Ray}}$
    end if
    Evaluate $\mathbb{C}_{\text{rate}} = \dfrac{\sum_{i=1}^{2^{N+1}} \text{count}_i[\mathbb{C}_{\text{rate}}^{l_1,l_2,\ldots,l_{N+1}}]_i}{\text{iteration}};$
    $\mathbb{P}_{\text{out}} = \dfrac{\sum_{i=1}^{2^{N+1}} \text{count}_i[\mathbb{P}_{\text{out}}^{l_1,l_2,\ldots,l_{N+1}}]_i}{\text{iteration}}$
  end for
  Evaluate $\mathbb{C}_{\text{rate}}^{\text{avg}}$ & $\mathbb{P}_{\text{out}}^{\text{avg}}$
end for

step, evaluate $\mathbb{I}_{\text{rate}}^{\text{avg}}$ and $\mathbb{P}_{\text{out}}^{\text{avg}}$. To check the performance of DA-NCC using the proposed channel model, network is simulated with the parameters given in Table 2. A model similar to the system model given in [5] is considered for the comparison purpose with appropriate changes to keep the fairness intact.

We compare the outage probability for different cases as a function of h_D in Fig. 10. It can be observed that if R is considered not to be energy constrained, then it does not need to harvest energy thus, providing all the RF energy to the information. Hence, in this case, we get the best results in terms of outage, that can act as an upper bound for reference. That is, we get the best performance when energy is not harvested. On the other hand, if R transmits at the harvested power only (using (14) and (27)), we get the worst performance as the power harvested depends upon the

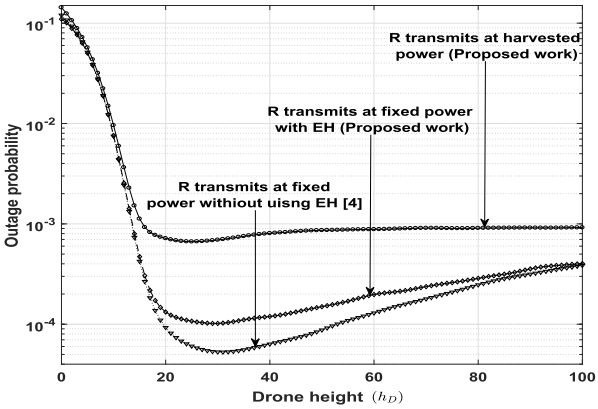

FIGURE 10. Outage probability w.r.t drone height (meter).

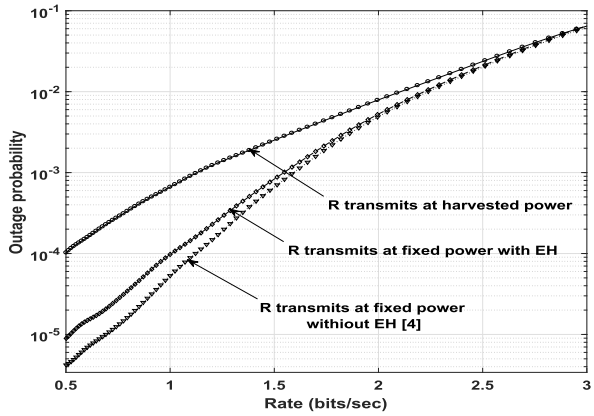

FIGURE 11. Outage probability w.r.t rate.

channel conditions too. Hence, R has less harvested power to transmit, thus, providing the worst performance. Finally, if R transmits with a fixed transmit power but also harvests energy (using only (27)) to maintain this fixed power, then we get relatively better performance. The performance of this scheme depends on the value of Ψ set in (2). It's worth noting for all the cases that initially as h_D increases, probability of occurrence of LoS also increases. Due to this, the path loss exponent decreases and because of smaller value of h_D, large scale attenuation has lesser effect on outage probability. As a result, performance of DA-NCC system improves. After an optimum drone height ($\approx$ 25-28 meters), path loss exponent decreases but due to increase in h_D, large scale attenuation increases. Hence, we see an increase in the outage probability.

Fig. 11 compares the outage performance of the cases considered in Fig. 10 with respect to rate. Similar logic can be applied as discussed for Fig. 10 in case of Fig. 11. The best outage performance is obtained when full power is conserved for IT (i.e R does not harvest energy). This worsens a bit when R transmits with fixed power and it's the worst when R transmits with variable harvested power as explained above.

Fig. 12 shows rate w.r.t h_D. The reason for the curves having different slopes for outage probability can again be explained as done before for Fig. 11. It can be observed here that, with an increase in h_D, the rate for all the considered

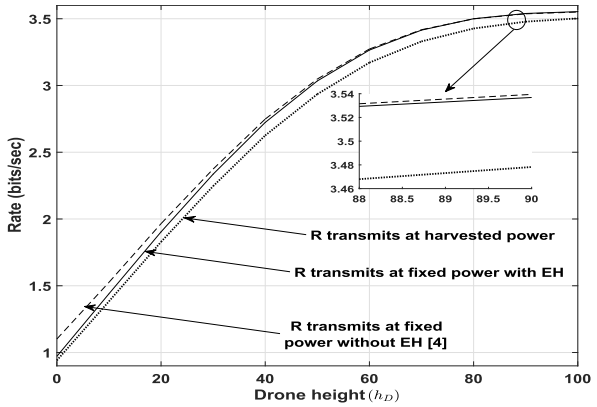

FIGURE 12. Rate w.r.t drone height (meter).

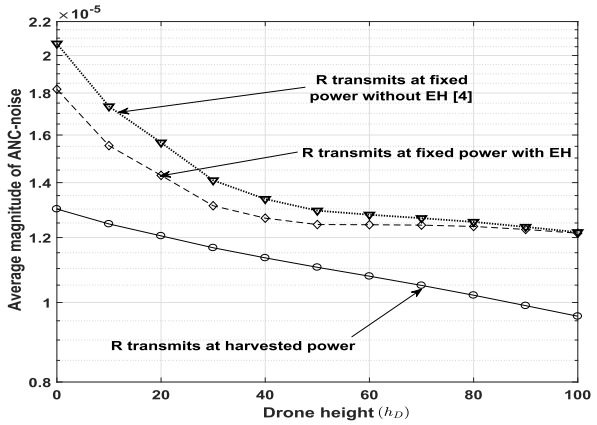

FIGURE 13. Average magnitude of ANC-noise w.r.t drone height (meter).

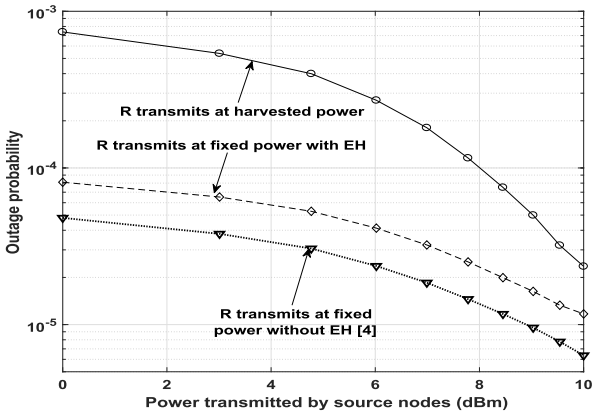

FIGURE 14. Outage probability w.r.t power transmitted by source nodes.

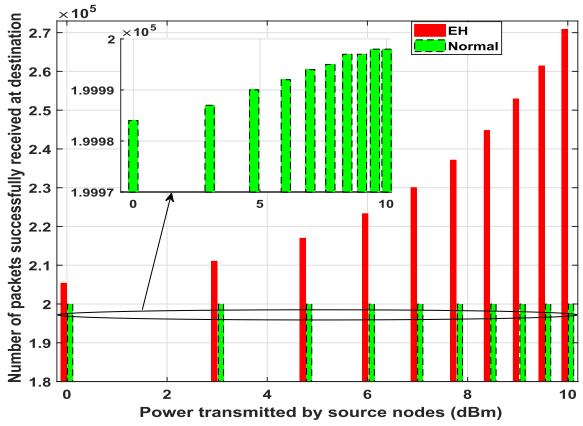

FIGURE 15. Number of packets received successfully at receiver w.r.t power transmitted by sources.

cases shows an increasing nature. However, the worst rate is obtained when R transmits using harvested power only. This is due to variation in the harvested power (based on channel parameters) during different sessions. Whereas, the value of rate is maximum when there is no EH at R because the entire RF power is allocated to IT which is not the case when R harvests energy.

Fig. 13 shows average magnitude of ANC-noise w.r.t h_D. Here it is noted that average magnitude of ANC-noise decreases as drone height increases for all the three cases. Average magnitude of ANC-noise is low in case when R transmits the coded signal at harvested energy and its value is high when R transmits the coded signal without using EH. This happens because in case of EH the signal power is splitting into two part. The first fraction associated with EH and the 2^{nd} portion associated with signal.

A plot between outage and power transmitted by source nodes is shown in Fig. 14. It can be observed here that, with an increase in power transmitted by source nodes, the outage probability for all the considered cases shows a decreasing nature. It may be noted from the outcome that the worst performance is obtained when R transmits at harvested power only due to variation in the harvested power (based on channel parameters) during different sessions. Whereas, even though R transmits at a fixed power in the other two schemes, it shows the best performance when there is no EH at R because the entire RF power is allocated to IT which is not the case when R harvests energy.

Fig. 15 depicts the number of packets received successfully at destination w.r.t power transmitted by S_i nodes. Here it is observed that as power transmitted by S_i increases, the number of packets received successfully at destination increases in both the cases. However, the number of packets received in case of EH is higher as compared to the non EH case due to increase in the harvested power at R with increase in $\mathcal{P}_{S_i}$. As a result, the power required from the main battery ($\mathcal{P}_R''$) to maintain the fixed $\mathcal{P}_R$ is lesser in the case of EH. While in case when no EH is considered, a fixed $\mathcal{P}_R$ is taken from the main battery which reduces the main battery quickly as compared to EH case. It may also be noted here that for a given $\mathcal{P}_{S_i}$, the number of communication cycles when considering EH is more as compared the scheme with no EH which improves the lifespan of the proposed network. From the outcomes from Fig. 14 and Fig. 15, we have concluded that even though the performance in terms of outage is relatively worse in case of EH but the higher number of packets received at the destination for EH case compensates it sufficiently.

VII. CONCLUSION

In this paper, we have proposed a dynamic power splitting factor for harvesting the energy at nodes in DA-NCC system. The dynamic nature of EH factor enhances the network lifetime by extracting more energy from RF signals when the channel conditions are favourable and lesser energy when it's not. Thus, the system maintains a better relationship between EH and IT. In order to accurately model the channel for dynamic EH factor at nodes, we have also introduced a generic probability based statistical channel model for modelling A2G links. Results obtained using this proposed model gives a better characterization of links in energy harvesting scenario by taking statistical independence of links into account. Here the harvested energy may not necessarily be sufficient to fulfil the entire energy requirement for the node, but it's contribution increases the lifespan of the node by increasing the number of transmission cycles. Extensive simulations show that our proposal enhances the lifespan of the proposed network. Analytical framework is developed for ANC-noise and variance of ANC-noise for the proposed channel model and EH. We derived the rate equation for the proposed channel model and EH. Algorithm 1 is developed to decide the A2G channels. Algorithms 2 and 3 are developed for harvesting the energy at relay and source nodes. Algorithm 4 evaluates the performance metrics (rate and outage probability) of our proposed work.

The generalized system model is applicable in many real-time scenario such as disaster management, IoT-based application, smart cities etc. in which drone acts as an aerial relay and thus, enhances the reliability of the ground users. Optimization of different parameters (drone altitude and power splitting factor etc.) of the proposed work can be considered as future work which can be beneficial for the next generation wireless systems. Additionally, finding the (approximated) closed form for the definitive expressions presented in this paper may be an insightful future work.

REFERENCES

[1] J. N. Laneman, D. N. C. Tse, and G. W. Wornell, "Cooperative diversity in wireless networks: Efficient protocols and outage behavior," *IEEE Trans. Inf. Theory*, vol. 50, no. 12, pp. 3062–3080, Dec. 2004.

[2] S. Katti, H. Rahul, W. Hu, D. Katabi, M. Medard, and J. Crowcroft, "XORs in the air: Practical wireless network coding," *IEEE/ACM Trans. Netw.*, vol. 16, no. 3, pp. 497–510, Jun. 2008.

[3] S. Sharma, Y. Shi, J. Liu, Y. T. Hou, S. Kompella, and S. F. Midkiff, "Network coding in cooperative communications: Friend or foe?" *IEEE Trans. Mobile Comput.*, vol. 11, no. 7, pp. 1073–1085, Jul. 2012.

[4] P. Kumar, S. Darshi, and S. Shailendra, "Impact of channel correlation on network coded cooperation with two sources," *Phys. Commun.*, vol. 47, Aug. 2021, Art. no. 101374.

[5] P. Kumar, P. Singh, S. Darshi, and S. Shailendra, "Analysis of drone assisted network coded cooperation for next generation wireless network," *IEEE Trans. Mobile Comput.*, vol. 20, no. 1, pp. 93–103, Jan. 2021.

[6] T. M. Hoang, B. C. Nguyen, P. T. Tran, and L. T. Dung, "Outage analysis of RF energy harvesting cooperative communication systems over Nakagami-*m* fading channels with integer and non-integer *m*," *IEEE Trans. Veh. Technol.*, vol. 69, no. 3, pp. 2785–2801, Mar. 2020.

[7] C. Abou-Rjeily and G. Kaddoum, "Free space optical cooperative communications via an energy harvesting harvest-store-use relay," *IEEE Trans. Wireless Commun.*, vol. 19, no. 10, pp. 6564–6577, Oct. 2020.

[8] F. Wang, S. Guo, Y. Yang, and B. Xiao, "Relay selection and power allocation for cooperative communication networks with energy harvesting," *IEEE Syst. J.*, vol. 12, no. 1, pp. 735–746, Mar. 2018.

[9] C. Qiu, Y. Hu, and Y. Chen, "Lyapunov optimized cooperative communications with stochastic energy harvesting relay," *IEEE Internet Things J.*, vol. 5, no. 2, pp. 1323–1333, Apr. 2018.

[10] K. Huang and E. Larsson, "Simultaneous information and power transfer for broadband wireless systems," *IEEE Trans. Signal Process.*, vol. 61, no. 23, pp. 5972–5986, Dec. 2013.

[11] Y. Ye, L. Shi, X. Chu, H. Zhang, and G. Lu, "On the outage performance of SWIPT-based three-step two-way DF relay networks," *IEEE Trans. Veh. Technol.*, vol. 68, no. 3, pp. 3016–3021, Mar. 2019.

[12] Y. Xu, C. Shen, Z. Ding, X. Sun, S. Yan, G. Zhu, and Z. Zhong, "Joint beamforming and power-splitting control in downlink cooperative SWIPT NOMA systems," *IEEE Trans. Signal Process.*, vol. 65, no. 18, pp. 4874–4886, Sep. 2017.

[13] V. Singh, R. Kumar, and Z. Wei, "Adaptive time-switching and power-splitting protocols for energy harvesting sensor networks with multiple relays," *Comput. Netw.*, vol. 179, Oct. 2020, Art. no. 107341.

[14] V. Singh and H. Ochiai, "An efficient time switching protocol with adaptive power splitting for wireless energy harvesting relay networks," in *Proc. IEEE 85th Veh. Technol. Conf. (VTC Spring)*, Jun. 2017, pp. 1–5.

[15] M. Mozaffari, W. Saad, M. Bennis, and M. Debbah, "Unmanned aerial vehicle with underlaid device-to-device communications: Performance and tradeoffs," *IEEE Trans. Wireless Commun.*, vol. 15, no. 6, pp. 3949–3963, Jun. 2016.

[16] C. You and R. Zhang, "3D trajectory optimization in Rician fading for UAV-enabled data harvesting," *IEEE Trans. Wireless Commun.*, vol. 18, no. 6, pp. 3192–3207, Jun. 2019.

[17] Z. Kang, C. You, and R. Zhang, "3D placement for multi-UAV relaying: An iterative Gibbs-sampling and block coordinate descent optimization approach," *IEEE Trans. Commun.*, vol. 69, no. 3, pp. 2047–2062, Mar. 2021.

[18] J. Tang, G. Chen, and J. P. Coon, "Secrecy performance analysis of wireless communications in the presence of UAV jammer and randomly located UAV eavesdroppers," *IEEE Trans. Inf. Forensics Security*, vol. 14, no. 11, pp. 3026–3041, Nov. 2019.

[19] M. M. Azari, F. Rosas, K.-C. Chen, and S. Pollin, "Ultra reliable UAV communication using altitude and cooperation diversity," *IEEE Trans. Commun.*, vol. 66, no. 1, pp. 330–344, Jan. 2018.

[20] P. Kumar, S. Darshi, and S. Shailendra, "Drone assisted device to device cooperative communication for critical environments," *IET Commun.*, vol. 15, no. 7, pp. 957–972, Apr. 2021.

[21] K. M. Rabie, B. Adebisi, and M.-S. Alouini, "Half-duplex and full-duplex AF and DF relaying with energy-harvesting in log-normal fading," *IEEE Trans. Green Commun. Netw.*, vol. 1, no. 4, pp. 468–480, Dec. 2017.

[22] P. V. Mekikis, A. S. Lalos, A. Antonopoulos, L. Alonso, and C. Verikoukis, "Wireless energy harvesting in two-way network coded cooperative communications: A stochastic approach for large scale networks," *IEEE Commun. Lett.*, vol. 18, no. 6, pp. 1011–1014, Jun. 2014.

[23] D. Bapatla and S. Prakriya, "Performance of energy-buffer aided incremental relaying in cooperative networks," *IEEE Trans. Wireless Commun.*, vol. 18, no. 7, pp. 3583–3598, Jul. 2019.

[24] D. N. K. Jayakody, T. D. P. Perera, A. Ghrayeb, and M. O. Hasna, "Self-energized UAV-assisted scheme for cooperative wireless relay networks," *IEEE Trans. Veh. Technol.*, vol. 69, no. 1, pp. 578–592, Jan. 2020.

[25] Z. Mobini, M. Mohammadi, and C. Tellambura, "Wireless-powered full-duplex relay and friendly jamming for secure cooperative communications," *IEEE Trans. Inf. Forensics Security*, vol. 14, no. 3, pp. 621–634, Mar. 2019.

[26] T. Li, P. Fan, and K. B. Letaief, "Outage probability of energy harvesting relay-aided cooperative networks over Rayleigh fading channel," *IEEE Trans. Veh. Technol.*, vol. 65, no. 2, pp. 972–978, Feb. 2016.

[27] Z. Zhou, M. Peng, Z. Zhao, W. Wang, and R. S. Blum, "Wireless-powered cooperative communications: Power-splitting relaying with energy accumulation," *IEEE J. Sel. Areas Commun.*, vol. 34, no. 4, pp. 969–982, Apr. 2016.

[28] S. Yin, Y. Zhao, L. Li, and F. R. Yu, "UAV-assisted cooperative communications with power-splitting information and power transfer," *IEEE Trans. Green Commun. Netw.*, vol. 3, no. 4, pp. 1044–1057, Dec. 2019.

[29] W. Wang, X. Li, M. Zhang, K. Cumanan, D. W. K. Ng, G. Zhang, J. Tang, and O. A. Dobre, "Energy-constrained UAV-assisted secure communications with position optimization and cooperative jamming," *IEEE Trans. Commun.*, vol. 68, no. 7, pp. 4476–4489, Jul. 2020.
[30] M. Ashraf, J.-W. Jang, J.-K. Han, and K. G. Lee, "Capacity maximizing adaptive power splitting protocol for cooperative energy harvesting communication systems," *IEEE Commun. Lett.*, vol. 22, no. 5, pp. 902–905, May 2018.
[31] S. Mondal, S. Roy, and S. Kundu, "Outage and throughput performance of a multihop network with an adaptive power splitting-based energy harvesting," *Int. J. Electron. Lett.*, vol. 9, no. 4, pp. 403–412, Oct. 2020.
[32] A. Esse, K. Abdullah, M. H. Habaebi, and H. A. M. Ramli, "Dynamic power splitting simultaneous wireless information and power transfer split receiver for wireless sensor networks," *IEEE Access*, vol. 9, pp. 129407–129416, 2021.
[33] M. T. Mamaghani and Y. Hong, "On the performance of low-altitude UAV-enabled secure AF relaying with cooperative jamming and SWIPT," *IEEE Access*, vol. 7, pp. 153060–153073, 2019.
[34] J. Wang, H. Zhai, Y. Fang, and M. C. Yuang, "Opportunistic media access control and rate adaptation for wireless ad hoc networks," in *Proc. IEEE Int. Conf. Commun.*, vol. 1, Jun. 2004, pp. 154–158.

PANKAJ KUMAR received the B.Tech. degree (Hons.) in electronics and communication engineering from Uttar Pradesh Technical University, Lucknow, India, the M.Tech. degree (Hons.) with specialization in digital communication from Dr. A. P. J. Abdul Kalam Technical University, formerly Uttar Pradesh Technical University, and the Ph.D. degree from the IIT Ropar. He is currently working as a Guest Faculty with the Department of Electronics and Communication Engineering, NSUT, Delhi, India. His research interests include, drone assisted cooperative networks, network coding, D2D communication, energy harvesting, and intelligent reflecting surface.

SAGNIK BHATTACHARYYA (Graduate Student Member, IEEE) received the B.Tech. degree in electronics and communication engineering from Techno India, Salt Lake (affiliated under MAKAUT, previously WBUT), in 2018, and the M.S.(R) degree in wireless communication and signal processing from the IIT Ropar, in 2021, where he is currently pursuing the Ph.D. degree with the Department of Electrical Engineering. His research interests include coded cooperative, cross layer techniques, and intelligent transportation systems.

SAM DARSHI (Senior Member, IEEE) received the B.Tech. degree (Hons.) in electronics and communication from M. J. P. Rohilkhand University, Bareilly, Uttar Pradesh, and the Ph.D. degree from the Department of Electronics and Electrical Engineering (EEE), IIT Guwahati, India. He is currently working as an Assistant Professor at the IIT Ropar, Punjab. Prior to joining IIT Ropar, he worked as a Faculty Member with the IIIT Guwahati. His research interests include almost all aspects of wireless communication with a special emphasis on infrastructure-less multi hop and relay networks, cooperative communication, next generation wireless networks, and intelligent transportation systems.

ASHWANI SHARMA (Member, IEEE) received the B.Tech. degree from the LNM Institute of Informations Technology, Jaipur, India, in 2010, the master's degree in technology and communication systems from the ETSIT, Technical University of Madrid (UPM), Spain, in 2013, and the Ph.D. degree from the University of Deusto, Bilbao, Spain, in 2015. He was a Junior Research Fellow at the Indian Institute of Technology, New Delhi, India, from 2010 to 2011, and a Visiting Training Fellow at the University of Kent, Canterbury, U.K., from May 2014 to August 2014. He is currently working as an Assistant Professor at the Indian Institute of Technology Ropar, India. His research works have been published in various international journals and conferences, such as IEEE TRANSACTIONS and Letters, IET journals, and Wiley letters. His current research interests include exploiting field forming techniques in antenna design for wireless power transmission, the IoT, and 5G.

AKRAM A. ALMOHAMMEDI received the B.Sc. degree in electronics engineering from Infrastructure University Kuala Lumpur, Malaysia, in 2012, the M.Sc. degree in electrical and electronics engineering majoring in computer and communication system from the Universiti Kebangsaan Malaysia, Malaysia, and the Ph.D. degree in wireless communications and networks engineering from University Putra Malaysia (UPM), in 2019. He is currently an Assistant Professor at the University of Karabuk (UNIKA), Turkey, as well as a Senior Researcher (remote-based) at South Ural State University (SUSU), Russia. His research interests include the Internet of Vehicle, the Internet of Things, multi-channel MAC, steganography, and wireless sensor networks.

VLADIMIR SHEPELEV received the Ph.D. degree from Chelyabinsk State Agroengineering University, Russia, in 2000. Since 2007, he has been working as a Technical Scientist with LLC NTK-Logistics Transport and Logistic Company. He is currently an Associate Professor at South Ural State University (SUSU). He is also working in a project entitled "Development of an Intelligent Digital Platform for the Management of Transportation Systems of Cities Based on Artificial Intelligence." He has published several articles, books, and patents. His research interests include the Internet of Things (IoT), real time traffic management, and the Internet of Vehicles (IoV).

SAMAR SHAILENDRA (Senior Member, IEEE) received the M.Tech. degree from IIT Delhi and the Ph.D. degree from IIT Guwahati. He is currently working as a Senior Standards Architect at Intel Corporation, Bengaluru. He is also serving as the Vice-Chair for the M2M Working Group of Telecommunications Standards Development Society, India (TSDSI). He has more than ten years of industry and academic experience. He has published several papers in various peer-reviewed international journals and conferences and filed several patents.